Journal of
Ceramic Science
and Technology

J. Ceram. Sci. Tech., **05** 01] 45-50 (2014)
DOI: 10.4416/JCST2013-00038
available online at: http://www.ceramic-science.com

Characteristics of Micro-Gold-Particle/Glass-Ceramic Composite from Post-Sintering Thermal Treatment

W. Yi[1], X. Sun[*1], D. Niu[2], X. Hu[3]

[1]Key Laboratory for Anisotropy and Texture of Materials (Ministry of Education), Northeastern University, Shenyang 110819, China
[2]School of Science, Northeastern University, Shenyang 110819, China
[3]School of Mechanical and Chemical Engineering, The University of Western Australia, Perth 6009, Australia

received November 9, 2013; received in revised form January 1, 2014; accepted February 15, 2014

Abstract

Microstructural characteristics of a gold-particle (GP)-reinforced glass-ceramic (GC) composite at the GP/GC interface were investigated before and after heat treatment at 900, 1100 and 1300 °C. The interfacial regions between the GP and GC exposed on the fracture surface and relevant chemical reactions were examined. The as-processed GC matrix had a nano-scaled biphasic microstructure, with isolated amorphous leucite phase evenly distributed in the continuous feldspar matrix. After the GP/GC composite was heated at 900 °C, the amorphous leucite phases were transformed into leucite crystalline phases. Au_2Si and Au_5Si_2 found at the GP/GC interface proved that chemical reactions had indeed occurred during composite processing. Fracture surface features around the GP and GP/GC interface were further examined after heat treatment at 1100 °C and 1300 °C, showing new compounds were produced during the process. Characterization techniques, including X-ray diffraction (XRD) and Field Emission Scanning Electron Microscopy (FESEM), incorporating X-ray microanalysis using Energy-Dispersive Spectrometry (EDS), were employed to study the GP/GC interface.

Keywords: Gold particle, glass-ceramic, interface, thermal treatment, chemical reactions

I. Introduction

Owing to their excellent aesthetical properties, chemical stability and biocompatibility [6–9], glass-ceramics (GC) are widely used in dental clinics as veneers or partial dental crowns formed by means of painting then firing, hot pressing or over-pressing on metal and ceramic dental crowns or substrates [1–5]. However, such layered composites exhibit abrupt changes in material properties such as strength, hardness and ductility across the interface, which can influence the reliability and lifetime of the dental implants, if these are not properly tailored.

It has been shown recently that brittle glass-ceramic can be effectively reinforced with micro-dental gold particles (GP) [10]. The optical property of the gold/glass-ceramic composite is different to the GC matrix owing to the addition of GPs, but it can be changed easily with a porcelain coating with similar physical properties to those of the GC. The GP/GC composite can be used to form dental crowns by itself, or used as an intermediate layer bridging the glass-ceramic veneer and metal substrate. The toughening and strengthening mechanisms of the GP/glass-ceramic composite have also been studied [11].

It is known that the crystallization processing of glass-ceramics is affected by the heat-treatment temperature and duration [12–18]. The objective of this study is to examine microscopic details at the GP/GC interfaces (exposed by means of polishing and on the fracture surface) after heat treatments at three different temperatures. In this way, the chemical reactions between the GP and GC matrix during the composite processing can be better understood, which is important for further development of new dental glass-ceramics composites and a better understanding of the interfacial toughening and strengthening mechanisms.

II. Experimental

(1) Glass-ceramic composite and heat treatment conditions

In this study, commercial dental glass-ceramic and dental gold alloy (Au-Pt-Pd) were used to fabricate the gold-particle-(GP)-reinforced glass-ceramic (GC) composite. Normally, the GC is available in the form of solid ingots or small bars, ready to press in dental laboratories by means of either hot pressing or over-pressing on metal or ceramic substrate. To make the composite, loose unsintered glass-ceramic powders (9 μm, PM9, VITA Zahnfabrik H. Rauter GmbH & Co. KG, Germany) were selected, and VITA indicated that the type of dental ceramic is leucite ($K_2O{\cdot}Al_2O_3{\cdot}4SiO_2$)-particles-reinforced feldspathic ($K_2O{\cdot}Al_2O_3{\cdot}6SiO_2$) glass-ceramic. Micro-irregular elongated GPs, measured in few hundreds of microns

* Corresponding author: xyz6527753@163.com

in length [10], were produced in-house from a dental gold bar (Type IV, Esteticor, Switzerland) using a standard dental laboratory hand-piece with a tungsten-carbide bur at a high speed. A uniform mix of GC powders with micro-GPs would produce a composite with a uniform microstructure. In this study, three different uniform mixes are used together to create a non-uniform composite structure.

Three-point-bend (3-p-b) bar samples with concentrated GPs at one side against tensile failure were prepared from non-uniform ingots consisting of three layers of different GP/glass-ceramic mixtures with 0, 5 and 10 wt% GP. Clearly, different sample geometry, e.g. a dental crown, and different desired GP location will require different GP distributions in the ingots, as the viscous flow of glass-ceramic through a narrow channel and the mold geometry will determine the final GP distribution and location. A commercial pressing furnace, EP5000 (Programat, Ivoclar Vivadent, Liechtenstein), for fabrication of ceramic dental crowns was used to sinter the trial ceramic/metal ingots at 1000 °C in vacuum for 20 minutes, and then hot-pressed into the pre-made pattern moulds through the channel (d = 1.5 mm). Then, the specimens were quickly cooled in air to room temperature. This hot pressing and fast cooling process requires the glass-ceramic and GP to have compatible melting temperatures for surface wetting, and matching coefficients of thermal expansion (CTE) to avoid cracking upon fast cooling. Concentrated GPs were positioned on one side of the specimens for more resistance against tensile failure. After they had cooled down, the specimens were ground and polished down to a sub-micron surface finish [11].

Based on the melting temperatures of GC and GP (Table 1), three different heat treatment temperatures were selected to investigate the surface characteristics of the composite for a given heat treatment condition. Composite samples of the first group were heated at 900 °C for 6 h in air so the glass phases contained in the composite would have enough time to transform into crystalline phases. Composite samples of the second group were heated at 1100 °C for 2 h in air, where the surface microstructure variations of both GC and GP during the heat process could be examined. Composite samples of the third group were heated up to 1300 °C in air, then cooled down immediately, to characterize the surface characteristics of both the GC matrix and GP. The physical states of the GC and GP at different heat treatment temperatures are shown in Table 2. After being heated at 900 °C, composite samples were manually polished down to sub-micron surface except for the fracture surface. Then, those samples were coated with platinum in vacuum with high voltage for conductivity. Those samples with thermal treatments at 1100 °C or 1300 °C were coated with carbon for conductivity in vacuum with high voltage.

Table 1: Melting temperatures of the gold alloy and glass-ceramic used in this study

Materials	Gold alloy	Glass-ceramic
Melting range [°C]	1160 – 1275	900 – 1000

Table 2: The physical states of glass-ceramic and gold particle at different heat treatment temperatures.

Materials	900 °C	1100 °C	1300 °C
Glass-ceramic	solid	liquid	liquid
Gold particle	solid	solid	liquid

(2) Analysis and characterization

X-ray diffraction (Empyren, PANalytic, the Netherlands) was used to analyze crystalline phases in the GP/GC composite surface before and after heat treatment. The microstructural details, such as the GP/GC matrix interface, the features of the GP and the morphology of the GC matrix after the thermal treatments were observed by means of Field Emission Scanning Electronic Microscopy (Zeiss 55, Germany). Element distributions along the interface between GP and GC matrix after heat treatments at 1100 °C and 1300 °C were analyzed with X-ray Energy Dispersive Spectrometry (EDS).

III. Results and Discussion

The XRD patterns of the GP/GC composite before and after 900 °C treatment were characterized and are shown in Fig. 1. Fig. 1b reveals that the original GP/GC composite contains feldspar, leucite, gold and Al_xAu_y, which was reported in our previous study [11]. The GC matrix in the composite without any heat treatment is composed mainly of glass phases (amorphous leucite and feldspar) and limited crystal phases (leucite and feldspar crystalline) owing to the fast cooling rate adopted in the composite fabrication process. Fig. 1a shows many peaks of anorthic feldspar crystals (PDF 01 – 089 – 8573) and tetragonal leucite crystals (PDF 00 – 003 – 0467). It indicates that glass phases of GC matrix (amorphous feldspar and amorphous leucite) were transformed into crystalline phases after the 900 °C heat treatment. Besides the expected XRD patterns of feldspar, leucite, Al_xAu_y and gold, silicon compounds (Au_xSi_y) are also revealed by means of the XRD analysis as shown in Fig. 1(a) for the heat-treated GP/GC composite in the GP concentration region. The existence of Au_2Si (PDF 00 – 040 – 1140), Au_5Si_2 (PDF 00 – 36 – 0938) and Al_2Au (PDF 03 – 065 – 8473), which were found at the GP/GC composite, proved further chemical reactions between GP and GC had indeed occurred during the composite heat treatment at 900 °C. It should be mentioned that some peaks in the XRD pattern of Au, Al_xAu_y and Au_xSi_y overlap and only very limited gold aluminum com-

pounds and gold silicon compounds exist at the interface between the GP and GC matrix. The fact that XRD peaks of Al_xAu_y and Au_xSi_y patterns were observed in Fig. 1a is not accidental as the GC matrix itself does not contain those compounds.

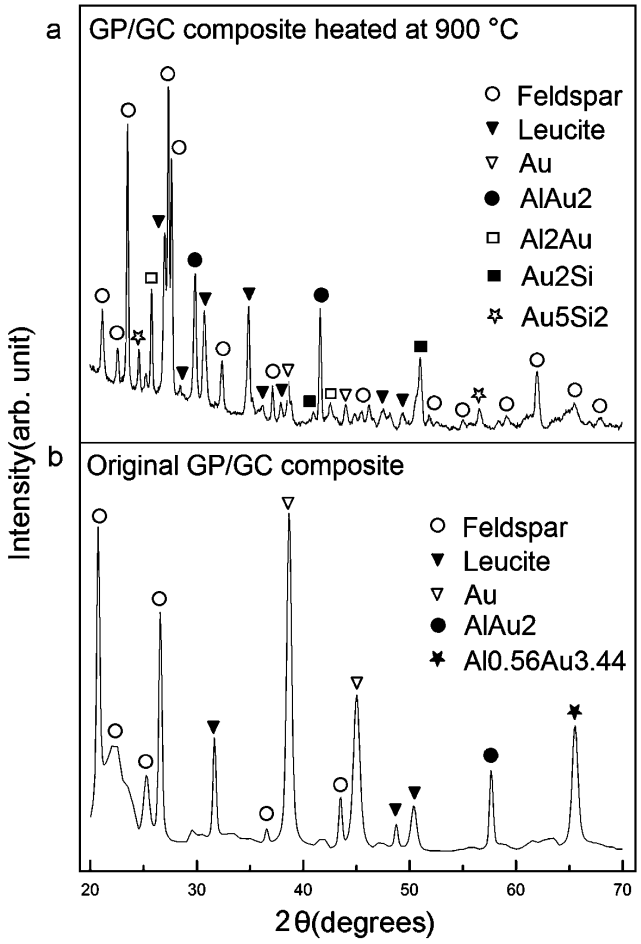

Fig. 1: XRD patterns of GP/GC composite before and after heat treatment at 900°°C: (a) heat-treated GP/GC composite; (b) original GP/GC composite.

A part of the micro-GP on the original composite polished surface is shown in Fig. 2a. The entire rugged boundary of the GP has been completely filled by the glass-ceramic matrix, and the interfacial regions are free of any form of pores or cracking. The nano-structures of the glass-ceramic matrix are clearly visible, which are much finer than the leucite glass-ceramic microstructures commonly reported in the literature [19–21]. After heat treatment at 900 °C for 6 h, many nano-scaled crystals are observed in the GC matrix, and the interface between the GP and GC matrix is also free of any cracking or pores in the polished surface of GP/GC composite, as is shown in Fig. 2b. The amorphous phase areas (Fig. 2a) were transformed into crystals as shown in Fig. 2b, which is consistent with the common glass-ceramic to crystalline transition after heat treatment [22–25]. Fig. 2c shows a fracture surface close to the interface between GP and GC, where the GP experienced large-scale plastic deformation failure, but is still mechanically interlocked into the ceramic matrix. Many isolated leucite nano-crystals emerged on the flat GC matrix fracture surface after the heat treatment. Crack-like patterns (indicated by the arrow) are observed on the GP, which normally do not exist on the pure GP surface, indicating brittle compounds at the GP/GC interface were formed during composite processing, which can be critical to strong interfacial bonding. Combined with the XRD pattern of the composite after heat treatment at 900 °C (Fig. 1a) and the morphology of those crack-like patterns, those new compounds are then inferred to be Al_xAu_y and Au_xSi_y.

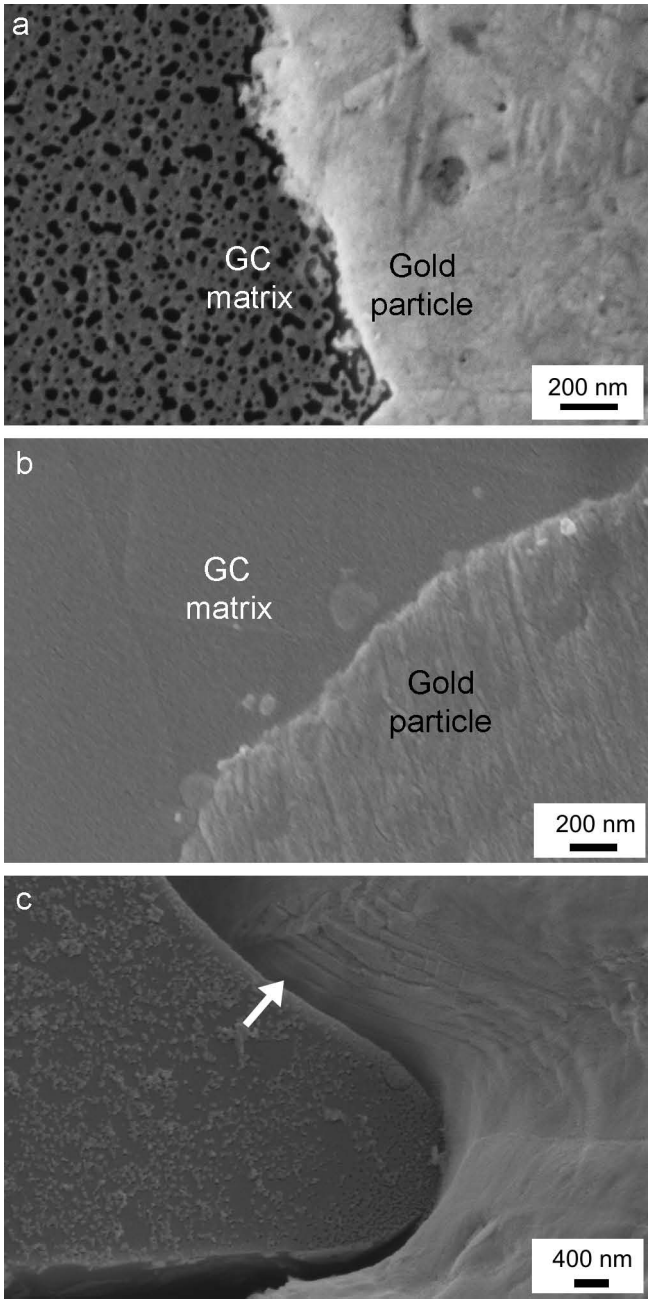

Fig. 2: (a) the original GP/GC composite polished surface shows a part of micro-GP in the biphasic GC matrix; GP/GC composite was heated at 900 °C for 6 h in air, (b) GC matrix features in polished surface show the amorphous phases were converted into the crystalline phase; (c) a plastically deformed GP on the fracture surface of composite, where several crack-like patterns on the GP surface were visible.

Fig. 3 shows an enlarged section of a composite fracture surface with a plastically-deformed GP during fracture after heat treatment at 1100 °C for 2 h in air, where many micro-sized oval-shaped terrace patterns with GP surface are observed and the "translucent region" (chemical reaction zone) along the interface is visible. The gray grain is a pore in the GP, which was fully filled by melted GC. Energy-Dispersive Spectrometry (EDS) was used to characterize the dominant elements at three different locations on the fracture surface. Spectrum (or position) 1 is within the glass-ceramic matrix near the interfacial region, showing the presence of Au as a result of the chemical reaction. Spectrum 2 is at the centre of GP fracture surface, showing Au is the dominant composition as expected. Spectrum 3 is on the side surface of GP, showing that Si and Au compositions are similar to those of Spectrum 1. The EDS results at Spectrum (or location) 1 and 3 indicate that the GP was not simply physically detached from the matrix owing to its large-scale plastic deformation, and a strong chemical bond did exist at the interface between GP and glass-ceramic matrix, and there were residual compounds left on the GP surface after debonding.

Surface features of a composite samples heat-treated at 1300 °C are shown in Fig. 4, where a number of crystals were located at the edge of a melted GP (Fig. 4a). Clearly, the melted GP had reacted with the GC matrix during the 1300 °C heat treatment, and as a result crystal-like microparticles were produced. The dark flat surface is GC matrix generated as a result of melting. Close to the arrow-indicated area of Fig. 4a, a number of crystals varying from around 100 nm to 1 μm and oval patterns emerged from the melted GP surface as shown in Fig. 4b. EDS was also used to characterize the dominant elements at two different locations on the melted composite surface. Spectrum (or location) 1 is within the oval patterns region, showing the presence of main elements of glass-ceramic i.e. Si, Al and O, associated Au the main composition of GP. Spectrum 2 located in the crystal surface shows the similar elements distribution to that in Spectrum 1, which proves the crystal had emerged from the oval patterns surface of the GP melted aggregation and those chemical reactions between GP and GC have been taken place during the heat treatment.

The GP surface had different patterns depending on the heat treatment conditions, the micro-sized terrace patterns at 1100 °C, and the micro-sized terrace patterns with protruding crystals at 1300 °C. It should be emphasized that a clean dental gold surface would not generate those oval-shaped terrace patterns or nano-crystals even after heat-treatment in air at those high temperatures. Furthermore, as GPs were melted to form more rounded GPs and GC was melted to be a flat matrix after 1300 °C heat treatment on the fracture surface, those micro-crystals on GP surface shown in Fig. 4b are completely different to the normal features of the pure dental gold and the glass-ceramic matrix, and hence they must be evolved from the residuals left on the GP surface from the previous chemical reactions during the manufacturing process. Therefore, chemical reactions between the GP and GC matrix must have occurred and there were residuals of chemical compounds on the GP side surface even after debonding and large-scale plastic deformation.

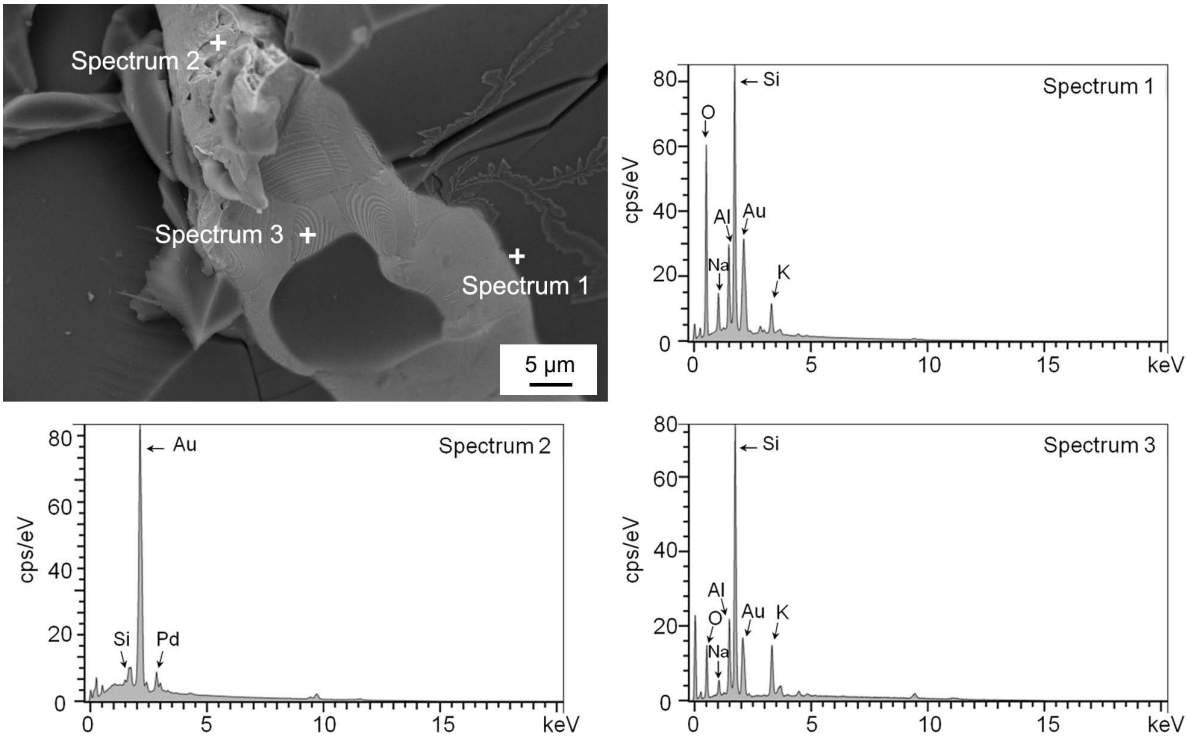

Fig. 3 : Composite sample with a plastically deformed GP on the fracture surface was heat-treated at 1100 °C for 2 h in air. Spectrum (or position) 1 is within the GC matrix near the metal/ceramic interface; Spectrum 2 is at the centre of GP fracture surface, and Spectrum 3 is on the oval-shape terrace patterns on the GP surface.

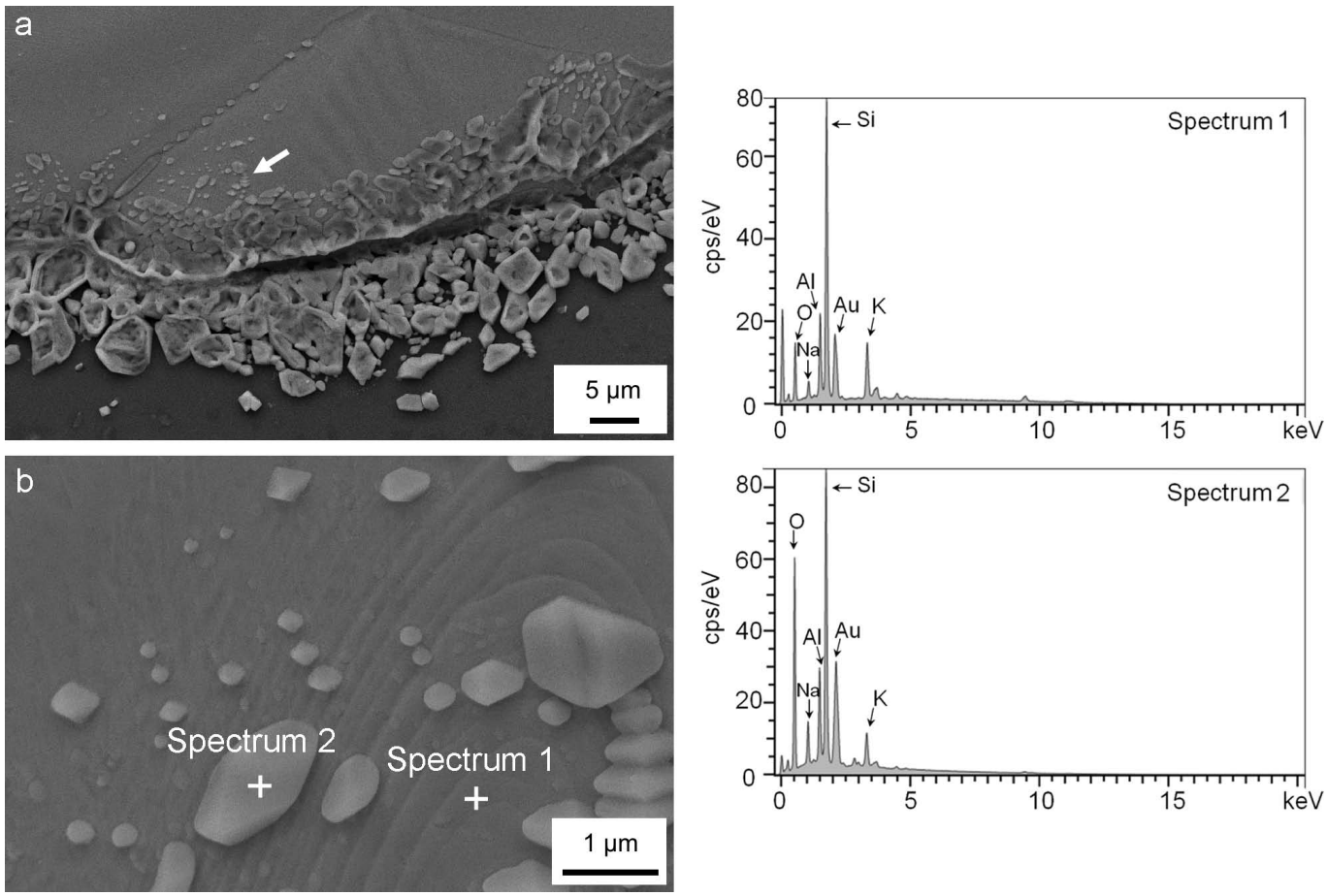

Fig. 4: Composite sample with GP exposed on a fracture surface was heated up to 1300 °C in air, and then cooled down. (a) Close-up around the edge of a melted GP, where the dark flat surface is GC matrix; (b) Close-up of (a), showing oval-shape terrace patterns and crystals from 100 nm to 1 μm were formed on the melted surface of the GP. Spectrum (or location) 1 is on the melted GP surface; Spectrum 2 is at the centre of one micro-crystal on the GP.

IV. Conclusions

Heat treatments of the fracture surfaces of the micro-GP-reinforced dental glass-ceramic revealed a number of important features on the interface between the GP and glass-ceramic matrix.

1. After six-hour heat-treatment at 900 °C, amorphous phase regions were transformed into crystals, and new compounds, Au_2Si, Au_5Si_2 and Al_2Au, were produced on the composite surface.
2. After two-hour heat-treatment at 1100 °C, the EDS results show that complex compounds of Au, Al, Si and O exist at the interfacial region between the GP and glass-ceramic matrix, and on the GP surface. Further chemical reactions of the compounds occurred during the heat treatment process, leaving nano-scaled features rarely observed on dental gold.
3. When the heat treatment temperature reached 1300 °C, the GPs were melted. Micro- and nano-crystals consisting Au, Al, Si and O elements emerged on the GP surface, indicating that chemical reactions between the GP and GC matrix had indeed occurred.
4. The chemical reactions between the GP and glass-ceramic are favorable as they lead to a strong chemical bond at the interface, essential for the strengthening and toughening mechanisms in the composite system.

Acknowledgements

This research was supported by the National Nature Science Foundation of China (50172030) and the Australian Research Council's Discovery Project Grant (DP1101052961). The authors are grateful for the technical assistance of the Centre for Microscopy, Characterization & Analysis at the University of Western Australia.

References

1 Verné, E., Fernández Vallés, C., Vitale Brovarone, C., Spriano, S., Moisescu, C.: Double-layer glass-ceramic coatings on Ti_6Al_4V for dental implants, *J. Eur. Ceram. Soc.*, **24**, 2699–2705, (2004).

2 Ballarre, J., López, D.A., Schreiner, W.H., Durán, A., Ceré, S.M.: Protective hybrid sol-gel coatings containing bioactive particles on surgical grade stainless steel: surface characterization, *Appl. Surf. Sci.*, **253**, 7260–7264, (2007).

3 Vitale Brovarone, C., Verné, A. Krajewski, E., Ravaglioli, A.: Graded coatings on ceramic substrates for biomedical applications, *J. Eur. Ceram. Soc.*, **21**, 2855–2862, (2001).

4 Yildirim, M., Fischer, H., Marx, R., Edelhoff, D.: *In vivo* fracture resistance of implant-supported all-ceramic restorations, *J. Prosthetic Dent.*, **90**, 325–331, (2003).

5 Höland, W., Rheinberger, V., Apel, E., Ritzberger, C., Rothbrust, F., Kappert, H., Krumeich, F., Nesper, R.: Future per-

spectives of biomaterials for dental restoration, *J. Eur. Ceram. Soc*., **29**, 1291 – 1297, (2009).

6 Kelly, J.R.: Ceramics in restorative and prosthetic dentistry, *Annu. Rev. Mater. Sci*., **27**, 443 – 468, (1997).

7 Conrad, H.J., Seong, W.-J., Pesun, I.J.: Current ceramic materials and systems with clinical recommendations: A systematic review, *J. Prosthet. Dent*., **98**, 389 – 404, (2007).

8 Höland, W., Rheinberger, V., Apel, E., van't Hoen, C.: Principles and phenomena of bioengineering with glass-ceramics for dental restoration, *J. Eur. Ceram. Soc*., **27**, 1521 – 1526, (2007).

9 Wang, Y., Katsube, N., Seghi, R.R., Rokhlin, S.I.: Statistical failure analysis of adhesive resin cement bonded dental ceramics, *Eng. Fract. Mech*., **74**, 1838 – 1856, (2007).

10 Yi, W., Hu, X., Ichim, P., Sun, X.: Processing and properties of pressable ceramic with non-uniform reinforcement for selective toughening, *Mater. Sci. Eng. A*, **558**, 543 – 549, (2012).

11 Yi, W. Hu, X.Z., Ichim, P., Sun, X.: Nano-scaled interface between micro-gold particles and biphase glass-ceramic matrix, *J. Am. Ceram. Soc*., **96**, 3662 – 3669, (2013).

12 Huang, S., Cao, P., Li, Y., Huang, Z., Gao, W.: Nucleation and crystallization kinetics of a multi-component lithium disilicate glass by *in situ* and real-time synchrotron X-ray diffraction. *Cryst. Growth Des*., **13**, 4031 – 4038, (2013).

13 Guo, X., Yang, H., Cao, M.: Nucleation and crystallization behavior of Li_2O-Al_2O_3-SiO_2 system glass-ceramic containing little fluorine and no-fluorine, *J Non-Cryst. Solids*, **351**, 2133 – 2137, (2005)

14 Erol, M., Genc, A., Öveçoğlu, M.L., Küçükbayrak, E., Taptik, Y.: Characterization of a glass-ceramic produced from thermal power plant fly ashes, *J. Eur. Ceram. Soc*., **20**, 2209 – 2214, (2000).

15 Karmakar, B., Kundu, P., Jana, S., Dwivedi, R. N.: Crystallization kinetics and mechanism of low-expansion lithium aluminosilicate glass-ceramics by dilatometry, *J. Am. Ceram. Soc*., **85**, 2572 – 2572, (2002).

16 Nguyen, T.P., Ip, J., Le Rendu, P., Lahamr, A.: Improved adhesion of gold coatings on ceramic substrates by thermal treatment, *Surf. Coat. Tech*., **141**, 108 – 114, (2001).

17 Darque-Ceretti, E., Hélary, D., Aucouturier, M.: An investigation of gold/ceramic and gold/glass interfaces, *Gold Bull.*, **35**, 118 – 129, (2002).

18 Katz, A., Nakahara, S., Geva, M.: *In situ* stress measurements of gold films on glass substrates during thermal cycling, *J. Appl. Phy.*, **70**, 7342 – 7348, (1991).

19 Cattell, M.J., Chadwick, T.C., Knowles, J.C., Clarke, R.L., Samarawickrama, D.Y.D.: The nucleation and crystallization of fine grained leucite glass-ceramics for dental applications, *Dent. Mater*., **22**, 925 – 933, (2006).

20 Chen, X., Chadwick, T.C., Wilson, R.M., Hill, R., Cattell, M.J.: Crystallization of high-strength fine-sized leucite glass-ceramics, *J. Dent. Res*., **89**, 1510 – 1516, (2010).

21 Fonseca, M., Silva, F., Ogasawara, T.: Study of the crystallization of leucite in feldspar glass matrix, *J. Therm. Analy. Calor*., **106**, 343 – 346, (2011).

22 Fernandez-Martin, C., Bruno, G., Crochet, A., Ovono Ovono, D., Comte, M., Hennet, L.: Nucleation and growth of nanocrystals in glass-ceramics: an *In Situ* SANS perspective, *J. Am. Ceram. Soc*., **95**, 1304 – 1312, (2012).

23 Dressler, M., Rüdinger, B., Deubener, J.: An *In Situ* high-temperature X-ray diffraction study of early-stage crystallization in lithium alumosilicate glass-ceramics, *J. Am. Ceram. Soc*., **94**, 1421 – 1426, (2011).

24 Ovono Ovono, D., Bruno, G., Pradeau, P., Berre, S.: Conditions for crystallization of LAS glass-ceramics as a function of nucleating agent amount and heat treatment, *Inter. J. Appl. Glass Sci*., **4**, 20 – 30, (2013).

25 Wondraczek, L., Pradeau, P.: Transparent hafnia-containing β-quartz glass Ceramics: nucleation and crystallization behavior, *J. Am. Ceram. Soc*., **91**, 1945 – 1951, (2008).